FHR-1395-3
PCD-TR-66-5
11 April 1966

Final Report

SOLAR FLARE HAZARD TO EARTH-ORBITING VEHICLES

Contract NAS 1-3601

Prepared For

National Aeronautics and Space Administration
Langley Research Center
Hampton, Virginia

FAIRCHILD HILLER
Republic Aviation Division
Farmingdale, L. I., New York 11735

SUMMARY

The object of this study has been to calculate the primary radiation incident on earth-orbiting vehicles during a solar flare. The effects of the earth's geomagnetic field have been taken into account, as well as those of a perturbing field due to the geomagnetic storm associated with a solar flare. Simple earth shadow effects have also been taken into account. Using this primary radiation as source function, dose rates for given orbits are then calculated using a computer routine. Dose rates are computed for typical orbits within a typical vehicle for the solar flares of February 23, 1956 and November 12, 1960.

TABLE OF CONTENTS

SECTION I - INTRODUCTION

The solar flare radiation hazard referred to in the title of this report is due to the increased solar cosmic radiation and the geomagnetic storm associated with a solar flare. The effect of the former in increasing the dose of a target is obvious, the second is due to the fact that a change in the earth's magnetic field results in a change in the natural magnetic shielding, thereby permitting particles of greater or lesser energy to arrive than during the "quiet" magnetic state.

In this study we assume that the distribution of the particles at large distances from the earth's field is isotropic, and an application of Liouville's Theorem tells us that the intensity of particles in any allowed direction is the same as at their starting point.[1] It therefore suffices to determine the allowed directions at the point in question. In the absence of magnetic effects other than that due to the earth's dipole, we assume that these are given by the classical Störmer theory, neglecting earth's shadow effects. In the presence of a magnetic disturbance, we assume that this allowed Störmer cone is modified. In order to calculate this modification on the same basis we must assume that the cylindrical symmetry of the problem is not broken, thus enabling a modified Störmer integral of the motion to be obtained. The geometric shadow due to the earth on the assumption of straight line trajectories is also included optionally in the coded analysis.

The theoretical analysis also allows us to obtain expressions for the cut-off rigidities for particles arriving from any direction at a point in the earth's magnetosphere.

The complete computer program therefore consists of three parts:

Part (1): A trajectory routine which supplies the orbit points for any required mission of the satellite or other vehicle at which the does rate is required

Part (2): The radiation environment routine which describes the differential energy flux of primary particles incident upon the vehicle

Part (3): A dose routine which calculates the dose rate at an interior point of the vehicle for the given mission in rads per orbit, given the vehicle's structure.

The report concludes with a series of graphs showing pictorially the results of these effects on the dose rate for a typical orbit during the two specific solar events of 23 February 1956 and 12 November 1960.

SECTION II - GEOPHYSICS DISCUSSION

A. GEOMAGNETIC DIPOLE MODEL

The coordinate system used later in the theoretical section of this report will be a geomagnetic system based on the eccentric dipole model. This assumes that the earth's magnetic field in the quiet state, i.e., in the absence of magnetic storms and ignoring the solar wind, is that due to a dipole whose center is placed at the point $\tau = 0.0685$ earth radii, longitude $\varphi = 150.9°$E, latitude $\lambda = 15.6°$N, and whose axis is tilted along the direction $\varphi = 68.9°$ $\lambda = 11.7°$. [2] These parameters are referred to in the computer program as T, α, β, η, ζ (T, alpha, beta, eta, zeta). The transformation from geographic to geomagnetic coordinates is thus achieved by

$$X_i'' = L_1(\zeta) L_2\left(\tfrac{\pi}{2} - \eta\right) L_3(T, \alpha, \beta) X_i$$

where:

$L_3(T, \alpha, \beta)$ performs a translation $(X, Y, Z) \rightarrow (X - T\cos\beta\cos\alpha,\ Y - T\cos\beta\sin\alpha,\ Z - T\sin\beta)$

$L_2\left(\frac{\pi}{2} - \eta\right)$ performs a rotation about the resulting Z axis by $\frac{\pi}{2} - \eta$ degrees,

$L_1(\zeta)$ performs a rotation about the resulting X axis by ζ degrees.

The resulting transformation from geographic coordinates X_i to geomagnetic coordinates X_i'' is

$$X'' = (X - T\cos\beta\cos\alpha)\sin\eta + (Y - T\cos\beta\sin\alpha)\cos\eta$$

$$Y'' = [-(X - T\cos\beta\cos\alpha)\cos\eta + (Y - T\cos\beta\sin\alpha)\sin\eta]\cos\zeta + (Z - T\sin\beta)\sin\zeta$$

$$Z'' = [(X - T\cos\beta\cos\alpha)\cos\eta - (Y - T\cos\beta\sin\alpha)\sin\eta]\sin\zeta + (Z - T\sin\beta)\cos\zeta$$

B. SOLAR FLARE PARTICLE RADIATION

Following Freier and Webber[3] we use the following two-parameter rigidity spectrum to describe the particle radiation occurring during a solar flare

$$J(>P) = J_0 \exp(-P/P_0)$$

Here $J(>P)$ is the integral intensity (particles/cm^2 - sec - ster) and P is the momentum per unit charge or rigidity. The parameters J_0 and P_0 are functions of time. The differential intensity spectrum is thus

$$dJ/dP = (-J_0/P_0)\exp(-P/P_0)$$

from which the differential energy fluxes may be obtained as

$$dJ/dT = (dJ/dP)(dP/dT)$$

or

$$dJ/dT = (dJ/dP)(T+m)/(T^2+2mT)^{1/2}$$

In Appendix I data are given for the flares of February 23, 1956 and November 12, 1960, and it is shown how analytic fits for the parameters $J_0(t)$ and $P_0(t)$ are obtained.

The manner in which these differential fluxes are used in the numerical routine is as follows. It is shown in the theoretical discussion later that the allowed directions of particle arrival at the target fill a cone, the Allowed Störmer cone, of solid angle Ω. On the assumption of isotropy and the use of Liouville's theorem as mentioned in the introduction, the flux impinging on the target, considered as a fictitious omni-directional flux, is therefore

$$J_{DC}(T,t) = (\Omega/4\pi)\, dJ/dT$$

and it is this number which gives the radiation environment; it is printed as out to the Computer Program of Part II. The other print-out is $J_{SF}(P,t) = \Omega(dJ/dP)$, which is used as an intermediate step in the calculation. This fictitious omni-directional flux is used only for dose calculations involving vehicles consisting of concentric spheres. In the general, non-symmetric case handled by the dose code, the correct flux $(\frac{4\pi}{\Omega} J_{DC})$, together with the allowed solid angle Ω, are the necessary input.

C. GEOMAGNETIC STORM MODEL

During a solar flare it is sometimes found that the plasma arriving at the earth brings with it a magnetic field, thus perturbing the quiet geomagnetic dipole field. (We ignore here higher moment effects, as well as the solar wind distortion.) The simple model we choose here is that of a uniform perturbing field, parallel or anti-parallel to the dipole field of the earth at the geomagnetic equator. We allow this field to vary with time, and the general variation is found to be as follows. During the initial part of the storm, the uniform field is such as to enhance that due to the earth's dipole at the equator. This is referred to as the Initial Phase in this report (sometimes it is divided into a sudden commencement SC and the initial phase IP). Later on this field becomes negative, and we enter upon the Main Phase (MP) of the storm (which is also sometimes subdivided into a main phase and a recovery phase).

As a uniform field extending to infinity is not a physical concept - indeed particles would be able to arrive at the earth only at the poles in such a model - we consider here only terminated fields for the two storm phases, following the model of Obayashi and Hakura.[4]

If we take a geomagnetic spherical polar coordinate system such that the earth's dipole may be represented by the vector potential

$$\underline{A} = [0, 0, M \sin\theta / r^2] \qquad (1)$$

then we may include an additional uniform field ΔH by putting

$$\underline{A}' = [0, 0, M\sin\theta/r^2 - \tfrac{1}{2}\Delta H r \sin\theta] \qquad (2)$$

We see that the total magnetic field at the point (r, ϑ, φ) is given by

$$\underline{H} = [2M\cos\theta/r^3 - \Delta H \cos\theta,\ M\sin\theta/r^3 + \Delta H \sin\theta,\ 0] \qquad (3)$$

We terminate this field by assuming either

(1) $H_r = 0$ at $r = r_0'$; i.e. $\Delta H = 2M/r_0'^3$ corresponding to the initial phase, or

(2) $H_\theta = 0$ at $r = r_0''$; i.e., $\Delta H = -M/r_0''^3$ corresponding to the main phase. (4)

In practice, for simplicity and uniformity of notation, we use the parameter r_0 to represent the addition field where

$$r_0 = (2M/\Delta H)^{1/3} \quad (5)$$

and may be positive or negative to represent both phases.

In Appendix II the analytic representation of the geomagnetic storm disturbance as a function of time is given, and the parameters fitting the curves to the known data of the storms of 23 February 1956 and 12 November 1960 are given. The computer program of Part 2 (Flux Environment Routine) also allows for a tabular input of geomagnetic storm ΔH values.

SECTION III - DISCUSSION OF THE THEORY

A. STÖRMER THEORY

We may write the Lagrangian for a charged particle of rest mass m_o in a magnetic potential $\underline{A}$ as [1]

$$\mathcal{L} = -m_o c^2 (1 - v^2/c^2)^{1/2} + (Ze/c)\, \underline{A} \cdot \underline{v} \qquad (1)$$

In the case of a potential given by

$$\underline{A} = [0,\ 0,\ A_\phi(r, \theta)] \qquad (2)$$

in the spherical coordinate system of IIC, the coordinate φ is ignorable, leading to the integral of motion

$$p_\phi = m_o (1 - v^2/c^2)^{-1/2} r^2 \sin^2\theta \dot{\phi} + \frac{Ze}{c} r \sin\theta A_\phi \equiv \Gamma \text{ (constant)} \qquad (3)$$

Defining the angle ω by $\cos\omega = r \sin\theta \dot{\phi}/v$, the angle which the velocity of the particle makes with the aximuthal direction, we have, putting $m = m_o(1 - v^2/c^2)^{-1/2}$,

$$\cos\omega = \Gamma / mrv\sin\theta - (Ze/mvc) A_\phi \qquad (4)$$

The conventional form of this integral of the motion in the case of a pure dipole field ($A\varphi = M\sin\theta/r^2$) is obtained by defining

$$l = (ZeM/mvc)^{1/2}$$

and

$$\gamma = \Gamma / 2mvl \qquad (5)$$

we may then use Störmer units $r_s = r/l$ to obtain

$$\cos\omega = 2\gamma / r_s \sin\theta - \sin\theta / r_s^2 \qquad (6)$$

The allowed regions in space are then those for which

$$|\cos\omega| \leq 1 \qquad (7)$$

The boundaries of such regions are those curves given by

$$|\cos\omega| = 1 \qquad (8)$$

or

$$2\gamma / r_s \sin\theta - \sin\theta / r_s^2 = \mp 1 \qquad (9)$$

Examples of these regions for various values of γ are given in Figure 1. Apart from the point ($r = 0$, $\theta = 0$) the boundaries cut the equator where $2\gamma/r - 1/r^2 = \pm 1$; a one-point pass connecting the outer and inner allowed regions exists when the boundary of the outer forbidden region (corresponding to $\cos\omega = +1$) cuts the equator at a double-point. This occurs for $\gamma = 1$.

The Störmer cone is that cone generated by the trajectories permitted to arrive at the point (r_s, θ) on the basis of equation 6. The surface of this cone will be generated by these particles which can just arrive at the point in question via a one-point pass; this corresponds to γ having its critical value $\gamma_c = 1$. The corresponding value of $\cos\omega$ is $\cos\omega_c = 2/(r_s \sin\theta) - \sin\theta/r_s^2$ and the solid angle of the allowed stormer cone is

$$\Omega = 2\pi(1 + \cos\omega_c) \tag{10}$$

It should now be noted that the Störmer cone is an upper limit to the allowed cone of trajectories insofar as all trajectories lying outside are definitely forbidden, but that not all trajectories within may eventually reach the point of interest, the earth's shadow, for example, being one of the factors precluding the arrival of some particles. Another factor is the geomagnetic penumbral effect, discussed in reference (1), where further references are cited. The geometrical earth's shadow, on the basis of straight line trajectories, may be allowed for by simply subtracting the solid angle the earth subtends at the point of interest. There is an option in Part 2 of the program enabling this to be done. If we neglect the earth's shadow the Störmer cone gives an upper limit to the particle radiation which may be received at a given point in space, and as such is a safe overestimate.

B. CUT-OFFS

On the basis of the above Störmer Theory we may calculate the minimum momentum which a particle must have to arrive at a point in space (r_e, θ_e), making an angle ω_e with the azimuth. At arrival we must have from (6)

$$\cos\omega_e = 2\gamma l/r_e \sin\theta_e - l^2 \sin\theta_e/r_e^2 \tag{11}$$

The geometrical parameters (r_e, θ_e, ω_e) thus relate the dynamical parameters (ℓ, γ) by

$$2\gamma = (\ell^2 + b)/a\ell \tag{12}$$

where

$$a = r_e / \sin^2\theta_e \tag{13}$$

$$b = r_e^2 \cos\omega_e / \sin\theta_e = r_e \cos\omega_e \, a \sin\theta_e \tag{14}$$

Throughout the trajectory (7) must hold; in fact, as discussed above, the particle will just arrive at the point of interest, arriving through the one point pass, if the outer boundary region determined by $\cos\omega = 1$ cuts the equator at a double point. Thus

$$(\ell^2 + b)/a r - \ell^2/r^2 = 1 \tag{15}$$

has a double root, where we have eliminated γ by (12). This occurs when $\ell = a + \sqrt{a^2 - b}$, where we choose the larger ℓ value, corresponding to minimum momentum. This gives the cut-off momentum for a simple dipole field

$$p(r_e, \theta_e; \omega_e) = \left|\frac{ZeM}{c}\right| \frac{\sin^4\theta_e}{r_e^2 [1 + (1 - \sin^3\theta_e \cos\omega_e)^{1/2}]^2} \tag{16}$$

Measuring momentum in BeV/c , distance in earth-radii, and using λ for geomagnetic latitude, we have the standard expression

$$p = (59.4\, Z/r^2) \cos^4\lambda \, [1 + (1 - \cos^3\lambda \cos\omega_e)^{1/2}]^{-2} \tag{17}$$

The quantities of particular interest are the cut-off momenta corresponding to $\cos\omega = -1$, $p_{c\ \min}$; $\cos\omega = 0$, $p_{c\ \text{vert}}$; and $\cos\omega = 1$, $p_{c\ \max}$.

It is noteworthy that the value of γ ($\ell^2 + b/2a\ell = 1$) is here independent of the momentum. This is not the case in general.

C. MODIFIED STÖRMER THEORY

We may proceed in a manner similar to that of the two previous sections when there is present an additional uniform magnetic field of the type described in IIC. The vector potential is now

$$\underline{A} = [0, 0, M\sin\theta/r^2 - \tfrac{1}{2}\Delta H \cdot r \sin\theta] \tag{18}$$

and the störmer integral IIIA (4) becomes

$$\cos\omega = 2\gamma l/r\sin\theta - \sin\theta\, l^2/r^2 + r\sin\theta\, l^2/r_0^3 \qquad (19)$$

using the parameter r_0 of IIC(5).

As before, the boundaries of the forbidden regions are given by $|\cos\omega| = 1$; on the equator these points are thus given by

$$2\gamma l/r - l^2/r^2 + r\, l^2/r_0^3 = \pm 1 \qquad (20)$$

or

$$f_\pm(r) \equiv (l^2/r_0^3)r^3 \mp r^2 + 2\gamma l r - l^2 = 0 \qquad (21)$$

As well as the inner forbidden region corresponding to the smallest positive root of $f_-(r) = 0$, and an intermediate forbidden region corresponding to the two smallest positive roots of $f_+(r) = 0$, we now have in addition an outer forbidden region corresponding to a root of $f_+(r) = 0$ for $r_0 > 0$ (Initial Phase) or $f_-(r) = 0$ for $r_0 < 0$ (Main Phase). Examples of the corresponding Störmer diagrams are given in Figure II. These outer forbidden regions play no role here, for it may be shown that they occur for $r > |r_0|$, i.e., beyond the point at which we assume our field to be terminated (Appendix IV).

The condition for a one point pass is now simply that the equation $f_+(r) = 0$ have a double root - the two smallest positive roots coinciding with the smallest positive root of $f_+(r) = 0$. Details of this method of determining the critical value of γ - which now depends on momentum - are given in Appendix IV.

D. MODIFIED CUT-OFFS

When we wish to calculate the cut-off momentum due to an additional uniform magnetic field in the presence of a dipole field, the method used is exactly analogous to that of B. The particle arrives at (r_e, θ_e) with azimuth angle ω_e giving

$$\cos\omega_e = 2\gamma l/r_e\sin\theta_e - l^2\sin\theta_e/r_e^2 + r_e\sin\theta_e\, l^2/r_0^3 \qquad (22)$$

The dynamical quantities (γ, ℓ) are thus related by

$$2\gamma = (\ell^2 + b)/a\ell \tag{23}$$

where

$$a = r_e[\sin^2\theta_e (1 - r_e^3/r_0^3)]^{-1} \tag{24}$$

$$b = r_e \cos\omega_e \sin\theta_e \, a \tag{25}$$

Throughout the trajectory

$$|\cos\omega| = |(\ell^2+b)/ar\sin\theta - \ell^2 \sin\theta/r^2(1 - r^3/r_0^3)| \leq 1$$

and the condition for a one-point pass is that this equation for $\cos\omega = 1$ should have a double root on the equator. As in Appendix IV we find that this equation

$$(\ell^2/r_0^3)r^3 - r^2 + \{(\ell^2+b)/a\}r - \ell^2 = 0 \tag{26}$$

has a double root when that root coincides with the lower positive root of the derived equation

$$(3\ell^2/r_0^3)r^2 - 2r + (\ell^2+b)/a = 0 \tag{27}$$

This double root is

$$r_{DBLE} = (r_0^3/3\ell^2)(1-\alpha) \tag{28}$$

where

$$\alpha = \{1 - (3/ar_0^3)\ell^2(\ell^2+b)\}^{1/2} \tag{29}$$

On substituting this double root into the original equation we have

$$\alpha^3 - 3/2\,\alpha^2 + 1/2 = 27\ell^6/2r_0^6 \tag{30}$$

which together with

$$\alpha^2 = 1 - 3\ell^2(\ell^2+b)/ar_0^3 \tag{31}$$

determines the value of α, and thus ℓ, corresponding to the cut off momentum required. For a numerical solution we eliminate ℓ between equations 30 and 31 to obtain the quartic in α

$$\alpha^4(1-A) - \alpha^3(1+2A-3B) - \alpha^2(3/4 - 1/2\,B) + \alpha(1/2+2A-3B+C) + (1/4+A-\tfrac{3}{4}B+\tfrac{1}{4}C) = 0 \tag{32}$$

where $A = -27a^3/4r_0^3$ $B = -9ab/2r_0^3$ $C = 27\,b^3/2r_0^6$ (Appendix V).

In the case of small perturbing fields ΔH, it is shown in Appendix V that the following analytic solution for the cut-off momentum at angle ω may be obtained

$$P_{(\Delta H)} = P_{(0)}\left[1 + \left(\frac{1+k}{k}\right)\frac{\Delta H r^3}{2M}\left\{(1+k)^2\cos^6\lambda - 1\right\}\right] \qquad (33)$$

where $k \equiv (1 - \cos\omega\cos^3\lambda)^{1/2}$ $(\cos\lambda \equiv \sin\theta)$; for vertical incidence this reduces to

$$P^{VERT}_{(\Delta H)} = P^{VERT}_{(0)}\left[1 + \frac{\Delta H r^3}{M}(4\cos^6\lambda - 1)\right] \qquad (34)$$

where $P_{(0)}$ is the appropriate cut-off in the absence of the field ΔH.

E. EARTH'S SHADOW EFFECT

It is a straightforward matter to take the earth's physical presence into account in the foregoing work if we assume that the solar particles move along straight lines within the allowed Störmer cone. We simply subtract those trajectories which intersect the geometrical shadow cone of the earth at the point of interest. This calculation is exhibited in Appendix III, and an option has been incorporated into the computer code for Part (2) to perform this modification numerically.

However, we know that in fact the incident particles do not, in general, move along straight lines, and so the above method is at best an approximation to the actual effect of the earth on the trajectories. Some justification for the straight line approach may be given by considering the motion of a particle in a region near the point of interest within which the earth's field may be considered uniform. Equating the Lorentz Force $e\ \underline{v} \times \underline{B}$ to the centripetal force for motion in a circle radius ρ, $mv_\perp^2/\rho$, leads to the well known expression for the radius of gyration $\rho = m\, v_\perp\, c/ZeB$ where $v_\perp$ is the component of velocity normal to $\underline{B}$. For a relativistic problem this becomes

$$\rho = (E_{ev}/300)(v_\perp/c)(1/B_{gauss}) \quad \text{cms}$$

where E_{ev} is the total energy of the particle in electron volts. This tells us that for a 1 BeV proton ($E_{ev} \doteq 2.10^9$) the maximum value for ρ is about 175 kms (and also that the earth's field may be considered a posteriori as uniform since it does not change appreciably within this distance). For typical satellite altitudes which are greater than 175 kms, protons of energy less than 1 BeV may be considered to move along field lines near the satellite. Now the earth's dipole field makes an angle α to the vertical given by

$$\tan \alpha = \tfrac{1}{2} \cot \lambda \qquad (\lambda = \text{geomagnetic latitude})$$

and so, except for the vicinity of the geomagnetic equator where the cut-off already prevents particles of the energies being discussed here from arriving, the solid earth's shadow may be considered as blocking off that half of the particles travelling along the field lines leaving the earth. This fraction, one half, is also the figure approximately arrived at on the basis of geometrical considerations.

The above viewpoint is not expected to be applicable to the higher energy galactic cosmic rays.

F. NON-DIPOLE EFFECTS

We consider now the manner in which the earth's magnetic field differs from that of a simple dipole. These effects are:

(1) Higher multipole terms with axial symmetry

(2) Non-axially-symmetric terms.

1. Higher Multipole Terms with Axial Symmetry

In general, the magnetic potential of the earth may be expressed as

$$V = \sum_{n=1}^{\infty} r_e \left(r_e/r\right)^{n+1} T_n \qquad (r = \text{radial distance, } r_e = \text{earth radius})$$

where

$$T_n = \sum_{m=0}^{n} \left(g_n^m \cos m\phi + h_n^m \sin m\phi\right) P_n^m(\theta) \tag{35}$$

Here, g_n^m and h_n^m are the gauss coefficients, φ is the geographic longitude, θ the geographic colatitude, and $p_n^m(\theta)$ are spherical harmonics (suitably normalized). The squared value of T_n averaged over the complete spherical surface is given by

$$|T_n|^2 = \sum_{m=0}^{n} \left[\left(g_n^m\right)^2 + \left(h_n^m\right)^2\right] / (2n+1) \tag{36}$$

Using the Gauss coefficients given by Finch and Leaton,[8] Quenby and Webber[9] tabulate the various terms (see Table on page 17). From this table it can be seen that the relative importance of the higher multipole terms diminishes as we go further out in the magnetosphere. The model chosen in this work - that of the eccentric dipole - is such that the quadrupole terms g_2^0, g_2^1, h_2^1 vanish, and so gives improved values over those of the table, which refer to a tilted dipole. Even in the latter case, however, the higher order terms noted do not amount to more than 20% of the dipole contribution at the earth's surface.

In order to account for higher multipole terms in the framework of the present theory, it would be necessary to assume that the cylindrical symmetry of the problem was not destroyed. We should thus retain only the θ dependence, and express the vector potential, in the notation of Section III-A, as

$$A\phi(r,\theta) = \sum_{m=1}^{\infty} M_m P_m^1(\theta) r^{-(m+1)} \tag{37}$$

The Stormer integral (IIIA-4) would still exist

$$\cos\omega = \frac{\Gamma}{mrv\sin\theta} - \frac{Ze}{mvc}\sum_{m=1}^{\infty} M_m P_m^1(\theta) r^{-(m+1)} \tag{38}$$

We may write this in dimensionless form as before, defining

$$\gamma = \Gamma/2mv\ell \quad , \qquad \ell = (ZeM_1/mvc)^{1/2} \quad , \qquad r_s = r/\ell \; ;$$

$$\cos\omega = 2\gamma/r_s\sin\theta - \sum_{m=1}^{\infty} k_m P_m^1(\theta) r_s^{-(m+1)} \tag{39}$$

We have defined $k_n = M_n/M_1\ell^{n-1}$.

If we wish to include a uniform perturbing field in addition, we must supplement the above integral by the term $r_s \sin\theta/r_{os}^3$,

where $r_{os} = r_o/\ell$, $\Delta H = 2M_1/r_o^3$

Δ H being the uniform perturbing field.

Thus, even in the next most simple case after the dipole, the Stormer integral for a quadrupole term becomes

$$\cos\omega = 2\gamma/r_s \sin\theta - \sin\theta/r_s^2 - 3k_2 \cos\theta \sin\theta/r_s^3 + r_s \sin\theta/r_s^3 \quad (40)$$

The following two additional complications are introduced:

(i) The equation is of higher order in r_s, making the determination of its roots, and thus the cut-off, more difficult.

(ii) The latitude symmetry in θ has been destroyed, and the Stormer jaws may not now be assumed to open on the equator.

In view of the fact that this approach retains the approximation of φ- symmetry, it does not seem worthwile to pursue it in the light of the increasing numerical complexity involved. We should not expect the error caused by neglecting the term $-3k_2\cos\theta \sin\theta/r_s^3$ in equation (4) to be more than 20% near the equator; near the poles the percentage error could be much greater due to the $\cos\theta$ term, but numerically the cut-offs are small in this region and so the difference will not be great. These estimates are substantiated by the numerical results of reference 9 (given in their table 2). We discuss this approach next.

2. Non-Axially-Symmetric Terms

One of the most important influences which destroy the axial symmetry of the earth's magnetosphere is that due to the solar wind. This causes the boundary of the magnetosphere to be distorted in the well-known manner of elongation on the night side and compression on the day side. In addition, the earth's field is not pure dipole in character, even well within the magnetosphere boundary, as indicated above. A semi-empirical method for calculating vertical cut-offs due to Quenby and Webber[9] is to replace the earth's dipole by an imaginary "best-fit" local dipole. Thus the vertical cut-off rigidity $P = M\cos^4\lambda /4r_e^2$ becomes $P_M = M\cos^4\bar{\lambda} /4r_e^2$, where the new latitude $\bar{\lambda}$ is defined by

$$\bar{\lambda} = \tan^{-1}\left[\frac{V_c + 0.52\Delta V}{2(H_c + 0.52\Delta H)}\right] \quad ;$$

V_c , H_c are the vertical and horizontal components of the dipole field at the point in question, ΔV, ΔH are the departures at that point from a pure dipole. Near the equator (latitudes $< 20°$) the expression for P_M is modified -

$$P_M = \frac{M}{4r_e^2}\left[1 + \frac{0.6\Delta H}{H_c}\right]\cos^4\bar{\lambda}$$

As this approach uses measured deviations from dipole of the surface field components, it is not expected to be adequate for the calculation of cut-offs further out in the magnetosphere. To do this a description of the field similar to that known on earth must be given. This would require either measured values, or a more adequate description of the interaction of the solar wind with the earth's magnetosphere than is presently available. However, it is not expected that the higher multipole terms will play an important role in this region, since they fall off more rapidly in value than the dipole term, as indicated in the following table.

We should expect there to be a region of space for which the methods we have used here to be least in error. Well within the solar wind-magnetosphere boundary we do not expect the distortion due to the solar plasma to be severe. This boundary may be estimated as

$$r_c = \left[B_0^2 / 4\pi m n v_s^2\right]^{1/6} r_e$$

where r_c, r_e are the magnetosphere cavity and earth radii respectively, m the proton mass, n the plasma density, v_s the velocity of the solar plasma, and B_o the equatorial magnetic field strength.[10] The value of $r_c = 10.7\ r_e$ results from magnetic field measurements. In addition, beyond $1.5\ r_e$ the non-dipole terms are 10% of the dipole contribution. Thus for radial distances r, such that $1.5\ r_e < r < 10\ r_e$, the description given earlier in this section should be adequate.

Relative Importance of Spherical Harmonic Terms *

% of V_1 (dipole)

Radial Distance	$\|V_2\|$	$\|V_3\|$	$\|V_4\|$	$\|V_5\|$	$\|V_6\|$	$\sum_{n=2}^{6} \|V_n\|$
1.0 r_e	10.4	5.9	2.8	0.9	0.4	20.4
1.2 r_e	8.7	4.1	1.6	0.4	0.2	15.0
1.5 r_e	6.8	2.6	0.8	0.2	0.1	10.5
2.0 r_e	5.2	1.5	0.3	0.1	0.1	7.1
3.0 r_e	3.5	0.7	0.1	0.1	0.1	4.3

r_e = 1 earth radius

$$V = \sum_{n=1}^{\infty} V_n$$

$$V_n = r_e(r_e/r)^{n+1} T_n$$

at distance kr_e, $|V_n| = (r_e/k^{n+1}) |T_n|$, where $|T_n|$ was given in Section F. Radial distances are measured from earth's center.

* This table taken from reference 9.

SECTION IV - THEORY AND EXPERIMENTAL OBSERVATIONS

The essential data necessary to evaluate the results of the present work are the following:

(1) Magnetic Field Values

(2) Cut-Offs

(3) Dose Rates and Flux Measurements

These measurements should be made simultaneously, and above the atmosphere to avoid the complication of secondary production. The flux measurements should be carried out at points where the isotropic radiation can be determined, i.e., the functions $J_0(t)$ and $P_0(t)$ of Section II-B which are the values when the magnetosphere plays no role, as well as at the mission points. It is not surprising that it is difficult to find in the literature at present missions fulfilling all these conditions. In addition, the conditions under which the dose measurements were performed must be simulated in the corresponding theoretical calculation, in order to make meaningful comparisons between theory and experiment. However, there have been missions during which subsets of the total required data have been obtained, and so it is possible to make a partial comparison with theory.

One of the experiments in which many of the required data were obtained was that of the satellite Injun I.[11] During this mission cut-offs, fluxes, and magnetic field values were measured for four distinct solar proton events. The cut-offs were determined by the arrival of 1 - 15 MeV protons from the vertical direction, in terms of the McIlwain parameter, L, which we may take as corresponding to geomagnetic latitude by

$$\lambda = \arccos L^{-1/2} \tag{41}$$

although this relation is strictly true for a pure dipole field only. The vertical cut-off momentum for protons,

$$P = 14.9 \cos^4 \lambda \ \text{BeV/c} \tag{42}$$

which follows from equation (17), putting $Z = 1$, $\tau = 1$, $\omega = \pi/2$, may in fact be more accurately written for the earth's field as [12]

$$P_o = 14.9 L_o^{-2} \tag{43}$$

If we take the typical kinetic energy of a proton in the 1-15 MeV group to be 12 MeV, corresponding to a momentum of about 150 MeV/c, we see that the undisturbed L_o value should be about 10, corresponding to $\lambda \simeq 71°$. During the geomagnetic storm periods we expect this value to be changed; the computer program herein developed would enable the exact calculation to be made. But we may estimate the effect of the geomagnetic main phase storm by using the approximate analytic expression (equation 34), which we now write as

$$P = 14.9 L^{-2}\left[1 - \frac{4\Delta H}{M} L^3\right] \tag{44}$$

where we have neglected 1 with respect to $4L^3$, and have taken a main phase, and therefore negative, uniform disturbing field. Since we are told the measured value of the cut-off is the same in both the disturbed and undisturbed cases, we obtain the relation between L and ΔH,

$$\Delta H = \frac{M}{4}\left[\frac{1 - L^2 L_o^{-2}}{L^3}\right] \tag{45}$$

Thus, the value of $L = 4.8$, observed on July 13, 1961, corresponds to a disturbance $\Delta H = 55\gamma$. which is consistent with the first observed main phase minimum. The later value $L = 3.4$ corresponds to $\Delta H = 177\gamma$, which is greater than the next main phase minimum observed, but nevertheless in the right direction. The purpose of the present computer program is to enable one to reproduce numerically the observed flux and cut-off values, given the correct input data.

It is more difficult to make meaningful comparisons with experiment for the dose rates. To do so requires a machine computation using the correct environment and shielding data. In addition, dose computations quoted in the literature may differ by factors of two or three or more, and confusion associated with the gathered data has resulted in measurements made by two or more groups being shown to be incompatible.*

* Quoted in Reference 14.

In the absence of detailed information concerning shielding and vehicle trajectory apart from the environmental data, it is impossible to make other than order of magnitude comparisons. We consider here two descriptions of the Solar Cosmic Ray Event of November 12, 1960, in addition to the one given herein; that of Masley and Goedeke[13] referred to as A, and that of Keller and Pruett,[14] referred to as B. We note first the differences in the assumed spectra from the following table.

	Peak Intensity(E > 30MeV) protons/cm^2/sec	Integrated Intensity(E > 30MeV) protons/cm^2
A	1.2×10^5	9.1×10^9
B	2.4×10^4	2.7×10^9

Some peak dose rates we have obtained are:

(i) No geomagnetic field present, 12 rads/100 minute orbit.

(ii) Maximum inclination (82° geomagnetic) in earth's dipole field, 2.5 rads/orbit

(iii) Above orbit, with additional geomagnetic field, 4 rads/orbit.

These values refer to a tissue point at the center of an aluminum sphere 1 cm thick (2.7 gm/cm^2).

The integrated doses given by A, for a sample of air within the shield, and by B for an integrated skin dose, are approximately 1000 rads and 150 rads, respectively, extrapolating their figures to a shielding thickness of 2.7 gm/cm^2. To estimate an integrated dose from our figures given above, we replace the actual storm by a 'peak' storm of duration (integrated intensity)/(peak intensity). For the figures given by A this amounts to about 21 hours, for B, 31 hours. The corresponding integrated doses, roughly obtained by multiplying either time period by the peak dose rate, are, for the environments of the previous paragraph:

(i) A 151 rads	(ii) A 31.5 rads	(iii) A 50 rads
(i) B 223 rads	(ii) B 46.5 rads	(iii) B 74 rads

We note that the order of magnitude obtained for the field-free dose is more in agreement with B.

We reiterate that a quantitative evaluation would require a machine computation with the relevant trajectory, environment, and shielding input data.

SECTION V - CONCLUSIONS

Some of the conclusions of this study may be drawn from the series of graphs with which this report ends. From the results therein depicted, we see that considerable changes in dose rate may occur as a result of the magnetic field disturbance during a geomagnetic storm. This effect, coupled with the already enhanced radiation present during a solar particulate storm, may lead to a greatly increased radiation dose experienced by personnel in an earth-orbiting vehicle. The biological and other effects of this solar flare hazard should be evaluated, where possible using safe overestimates of the radiation involved.

The results on the non-concentric spherical shell vehicle indicate that weight saving may be achieved by taking advantage of the directionality of the radiation, without losing any effective shielding protection. (See Table IV)

The above deductions only apply within the framework of the magnetic field model chosen, i.e., a uniform magnetic disturbance superimposed on the earth's dipole and parallel or anti-parallel to it. In general, the disturbance will not be of such a simple nature. In addition, the effects of the Solar Wind have been disregarded; it is known that this plasma stream produces a continual distortion of the earth's dipole field, and is not representable by a uniform field parallel to the dipole.

Therefore, although the changes of dose rate obtained in the situation here considered are as anticipated, it would seem that a desirable refinement of the above approach would use a more realistic magnetic field configuration. It would be of interest to compare this better approximation to the physical situation with the results of this present study.

APPENDIX I

DATA FOR SOLAR FLARE PARTICULATE RADIATION

The particulate radiation during solar flare storms is parametrized as in IB,

$$J\ (>P) = J_o \exp(-P/P_o).$$

The behavior of the functions $J_o(t)$ and $P_o(t)$ associated with the solar storms of November 12, 1960 and February 23, 1956 is obtained as follows.

It is assumed that these functions can be fitted by the following expressions:

$$J_o(t) = \text{antilog}\ \left\{F_1,\ m - A(t - t_m)^2\right\} \qquad t \leq t_q$$

$$= \text{antilog}\ \left\{F_2,\ o - S(t + t_o)\right\} \qquad t > t_q$$

$$P_o(t) = \text{antilog}\ \left\{G_1,\ o - S_1(t + t_o)\right\} \qquad t \leq t_{qp}$$

$$= \text{antilog}\ \left\{G_2,\ o - S_2(t + t_o)\right\} \qquad t > t_{qp}$$

For smooth fitting of the parts of the $J_o(t)$ curve, we impose the conditions

$$F_{1,m} - A(t_q - t_m)^2 = F_{1,o} - S(t_q + t_o)$$

$$2A(t_q - t_m) = S$$

and for continuity of the $P_o(t)$ curve, $G_{1,o} - S_1(t_{qp} + t_o) = G_{2,o} - S_2(t_{qp} + t_o)$.

The parameters corresponding to the two storms dealt with here are given in the following table, Table I.

Table I

Particulate Radiation Parameters

	November 12, 1960	February 23, 1956
$F_1 m$	3.716	2.146
A	1.55×10^{-6}	3.18×10^{-6}
t_m	1050	600
t_q	1226	638
$F_{2,o}$	4.173	2.295
S	5.47×10^{-4}	2.41×10^{-4}
t_o	-300	0
$G_{1,o}$	2.389	2.623
t_q	1552	0
G	2.086	2.623
S_1	2.95×10^{-3}	2.41×10^{-4}
S_2	5.3×10^{-5}	2.41×10^{-4}

APPENDIX II

GEOMAGNETIC STORM REPRESENTATION

We shall fit the Initial Phase by a parabola. We shall arbitrarily divide geomagnetic storms into Great Storms and Lesser Storms, the criteria being that the Main Phase should exceed 100 γ in magnitude for the former. Following a suggestion of Akasofu et al, [5] to the effect that the Main Phases of Great Storms seem to consist of a constant plus a variable part, we fit a Lesser Storm Main Phase by one curve of the form $y = - axe^{-x/b}$, and that of a great storm by the sum of two such curves, one of which is invariable for all great storms and corresponds to a -100γ Main Phase maximum.

The input parameters necessary are; ΔH_i (Initial Phase Maximum in gammas), t_i (duration in minutes of the Initial Phase), ΔH_m (Main Phase Minimum in gammas), t_m (time of occurrence of Main Phase Minimum after commencement of geomagnetic storm, in minutes). In addition the computer program requires $t_{o(mag)}$, the time in minutes when the geomagnetic storm starts with reference to zero as the beginning of the Particulate Radiation Storm, and ΔX, Δx_{fin} giving the spacing of the time points and final time value, in minutes, respectively.

The analytical expressions are:

1. Lesser Storms $|\Delta H_m| \leq 100\gamma$

   (i) Initial Phase $\Delta H = (\Delta H_i/t_i^2)(t_i t - t^2) \qquad t \leq t_i$

   (ii) Main Phase $\Delta H = -2.7\{\Delta H_m/(t_m - t_i)\}(t - t_i)\exp\{(t_i - t)/(t_m - t_i)\}, \quad t > t_i$

2. Greater Storms $|\Delta H_m| > 100\gamma$

The Initial Phase fit is exactly as above. The main phase is assumed to be given by a curve of the form $y = .453\, xe^{-x/600} + Axe^{-x/x_o}$, where $y = - \Delta H$ and x is $t - t_i$.

The first portion on the right hand side has a maximum of 100 at $x = 600$. If $t_m - t_i < 600$, as is generally the case, we have a maximum at x_o approximately, say $x_m = x_o(1 \pm \delta)$. Putting in the condition $y'(x_m) = 0$, for small δ we get

$$\delta = (1 - x_o/600) / \{2.21 A \exp(x_o/600 - 1) + x_o/600\ (2 - x_o/600)\}$$

We may thus find δ by the approximation $x_o = x_m$, and the approximate value for A,

$$A = (e/x_m)\{|\Delta H_m| - .453\, x_m \exp(-x_m/600)\}$$

obtained by putting $y = |\Delta H_m|$ for $x = x_m$. A more accurate value of A, B, may be obtained from the newly found $x_o = x_m(1 - \delta)$, by putting $y = |\Delta H_m|$ for $x = x_o$,

$$B = \{|\Delta H_m| - .453 x_m \exp(-x_m/600)\} / \{x_m \exp(-1/1-\delta)\}$$

The form chosen for the main phase of the Great Magnetic Storms is thus

$$\Delta H = -.453(t - t_i) \exp\{-(t-t_i)/600\} + B(t-t_i)\{\exp\{-(t-t_i)/t_o\}$$

The parameters chosen to represent the geomagnetic sotrms present during the Solar Flares of February 23, 1956 and November 12, 1960 are given in Table II.

TABLE II

Geomagnetic Storm Parameters*

	23 February 1956	12 November 1960
ΔH_i	25	50
t_i	100	120
ΔH_m	-300	-300
t_m	400	480
$t_{o(mag)}$**	338	378

* Data for both storms in solar Proton Manual, edited by F. Frank McDonald, Appendix B, Graph of February Storm in Reference 5.

** These are the values used in the computer routine for effective comparison with the geomagnetic storm free case. In actual fact, the February geomagnetic storm occurred about two days after the particulate storm.

APPENDIX III

GEOMETRICAL SHADOW OF EARTH

There are essentially only three cases to consider, corresponding to diagrams A, B, and C of Figure IV.

Case A: $0 < \omega \leq \frac{\pi}{2} - \beta \qquad \cos\omega \geq \sin\beta$

In this case the earth's geometrical shadow cone is totally within the allowed cone, and the expression for the effective allowed solid angle is given by

$\Omega_{eff} = \Omega_{ST} - \Omega_{SH}$, in an obvious notation;

or $\Omega_{eff} = 2\pi(1+\cos\omega) - 2\pi(1-\cos\beta) = 2\pi(\cos\omega + \cos\beta)$

Case B: $\pi \geq \omega \geq \pi/2 + \beta \qquad \cos\omega \leq -\sin\beta$

In this case the earth's geometrical shadow cone is totally outside the allowed cone, and so does not alter the allowed solid angle, $\Omega_{eff} = \Omega_{ST}$.

Case C: $\pi/2 - \beta < \omega < \pi/2 + \beta \qquad \sin\beta > \cos\omega > -\sin\beta$

In this final case the earth's geometrical shadow cone and the allowed cone have a common solid angle, and the resultant effective angle is given by

$$\Omega_{eff} = \Omega_{ST} - \Omega_{COM}$$

where

$$\Omega_{COM} = 2\sin\beta \int_{-\cos\omega/\sin\beta}^{1} \arctan\left[\sqrt{1-\nu^2}\,\tan\beta\right] d\nu$$

We may evaluate this integral as follows; define $\nu = (\cos\omega / \sin\beta)$ and consider the indefinite integral

$$I = \int \arctan\left[\sqrt{1-\nu^2}\,\tan\beta\right] d\nu$$

From the transformation $x = \sqrt{1-\nu^2}\,\tan\beta$, we get

$$I = -\frac{1}{a}\int \tan^{-1}x\,(a^2-x^2)^{-1/2}\,x\,dx \qquad a \equiv \tan\beta$$

Integrating by parts,

$$I = \tfrac{1}{a}\tan^{-1}\{x\sqrt{a^2-x^2}\} + \tfrac{1}{a}\tan^{-1}\left\{\frac{x}{\sqrt{a^2-x^2}}\right\} - \frac{\sqrt{a^2+1}}{a}\tan^{-1}\left\{\frac{x\sqrt{a^2+1}}{\sqrt{a^2-x^2}}\right\}$$

Now

$$\Omega_{COM} = 2\sin\beta\left[I_{\nu=0}^{\nu=\gamma} + I_{\nu=0}^{\nu=1}\right]$$

$$= 2\sin\beta\left[I_{x=a}^{x=a\sqrt{1-\gamma^2}} + I_{x=a}^{x=0}\right]$$

Thus

$$\Omega_{COM} = 2\pi(1-\cos\beta) + 2\cos\omega \arctan\left[\sqrt{1-\frac{\cos^2\omega}{\sin^2\beta}}\tan\beta\right]$$

$$-2\arctan\left[\sqrt{\frac{\sin^2\beta}{\cos^2\omega}-1}\sec\beta\right] + 2\cos\beta\arccos\left[\frac{\cos\omega}{\sin\beta}\right]$$

For points near the earth's surface $\beta = \pi/2 - \delta$, where δ is small, and the effective allowed solid angle reduces to

$$\Omega_{eff} = \pi(1+\cos\omega) + \delta(\pi + 2\arcsin(\cos\omega))$$

We reiterate that the effective Störmer cones calculated here are only valid when the trajectories of the particles considered are straight lines in the vicinity of the point of interest.

APPENDIX IV

MODIFIED THEORY OF FORBIDDEN REGIONS

(i) INITIAL PHASE

Here $r_0 > 0$, and the equation determining the points where the boundaries of the forbidden regions cut the equator is

$$f_\pm(r) \equiv (\ell^2/r_0^3)r^3 \mp r^2 + 2\gamma\ell r - \ell^2 = 0 \tag{1}$$

These functions have extremal values where

$$f_\pm'(r) \equiv (3\ell^2/r_0^3)r^2 \mp 2r + 2\gamma\ell = 0 \tag{2}$$

i.e. at the points

$$\beta_\pm = (r_0^3/3\ell^2)(1 \pm \alpha) \tag{3}$$

$$\bar{\beta}_\pm = -(r_0^3/3\ell^2)(1 \pm \alpha) \tag{4}$$

where

$$\alpha = (1 - 6\gamma\ell^3/r_0^3)^{1/2} \tag{5}$$

and β ($\bar{\beta}$) refers to $f_+(r)$ ($f_-(r)$). The curves $f_\pm(r)$ have the general form of Figure III-i, from which we see that it is the curve $f_+(r)$ which determines the outer forbidden region. A one-point pass corresponds to the lowest root of $f_+(r) = 0$ being double, or

$$f_+(\beta_-) = 0 \tag{6}$$

i.e.

$$g(\alpha) \equiv \alpha^3 - \tfrac{3}{2}\alpha^2 + \tfrac{1}{2} - 27\ell^6/2r_0^6 = 0 \tag{7}$$

This equation has a root α_c, $0 < \alpha_c < 1$ for $r_0 > \sqrt{3}\,\ell$, whence the critical value of γ may be determined by

$$\gamma_c = (r_0^3/6\ell^2)(1 - \alpha_c^2) \tag{8}$$

We note that this is consistent because the double root β_- does occur on the equator within the field region determined by r_0. To prove this, note that

$$\beta_- = (r_0^3/3\ell^2)(1-\alpha) = \{3\ell^2/(2\alpha+1)\}^{1/2}$$

since $(1-\alpha)^2(\alpha+\tfrac{1}{2}) = 27\,l^6/2r_0^6$, or

$$\beta_- = (2\alpha+1)^{-1/2}\sqrt{3}\,l < r_0$$

In addition the greatest root of f+(r) occurs after the extremal β_+ ; but

$$\beta_+ = (r_0^3/3l^2)(1+\alpha) > r_0$$

and so we are beyond the region of the uniform field. This is the justification for the statement at the end of III C to the effect that the outer forbidden region plays no role.

For $r_0 < \sqrt{3}l$, we define the critical value of γ by $\gamma_c = \frac{1}{2} r_0$, noting that the sole positive root of f+(r) is r_0, $f+(r_0) = 0$.

(ii) MAIN PHASE

When $r_0 < 0$, the relevant double root occurs at

$$\beta_- = (|r_0|^3/3l^2)(\alpha-1)$$

The determining equation for α, (7), remains unchanged, but now there is always a root $\alpha_c > 1$ leading to a positive value of $\gamma_c = (|r_0|^3/6l^2)(\alpha_c^2-1)$.
Again we note that this root occurs in the field region which now is determined by

$r \le r_0'' \equiv 2^{-1/3}|r_0|$ (recall the definition of the terminated field for the main phase, II C (4), (5).) To prove this, we must show that

$$(|r_0|^3/3l^2)(\alpha-1) \le 2^{-1/3}|r_0|$$

or

$$(\alpha-1) \le 3\cdot 2^{-1/3}\, l^2/|r_0|^2$$

or equivalently that

$$\alpha^3 - 3\alpha^2 + 3\alpha - 1 \le 27l^6/2r_0^6$$

But from (7)

$$\alpha^3 - 3/2\,\alpha^2 + 1/2 = 27l^6/2r_0^6$$

so we must show that $-\frac{3}{2}\alpha^2 + 3\alpha - \frac{3}{2} \equiv -\frac{3}{2}(\alpha-1)^2 < 0$, which is true.

APPENDIX V
CUT-OFFS

In this section we determine analytic expressions for the cut-off momentum for the arrival of a particle at a point (r, λ) with angle ω to the east-west direction, in a magnetic field configuration consisting of the earth plus a uniform perturbing field, ΔH, along the dipole axes.

In the absence of the field ΔH, it was shown in III B that the cut-off momentum is given by $P_{(o)} = 59.4 / \ell_o^2$ BeV/C, where ℓ_o is the greater root of the equation

$$\ell^2 - 2a_o \ell + b_o = 0 \qquad a_o = r \sec^2\lambda \quad b_o = r^2 \cos\omega \sec\lambda \tag{1}$$

and the zero suffices refer to the absence of the uniform field ΔH.

In the presence of a uniform field ΔH, the cut-off momentum is again determined from the Störmer length ℓ, now obtained as a root of the simultaneous equations given in III-D. These are

$$(\alpha-1)^2(\alpha+\tfrac{1}{2}) = 27\ell^6/2r_0^6 \tag{2}$$

$$(\alpha-1)(\alpha+1) = -(3\ell^2/ar_0^3)(\ell^2+b) \tag{3}$$

where the parameter $r_0 \equiv (2M/\Delta H)^{1/3}$

Eliminating r_0, $$(\alpha+1)^2/(\alpha+\tfrac{1}{2}) = (2/3a^2)(\ell^2+b)^2/\ell^2 \tag{4}$$

When $r_0 = \infty$ we have the unperturbed Störmer case $\Delta H = 0$, for which the solution $\alpha = 1$ exists. This leads to the equation (1) for ℓ_o noted above, by substituting in (4).

When r_o is large we assume that a solution $\alpha = 1 + \varepsilon$ exists, where ε is small. The values of a and b are now changed from their unperturbed values a_o and b_o, to

$$a = a_o(1 - r^3/r_0^3)^{-1} = a_o(1+\delta)$$

$$b = l_0(1 - r^3/r_0^3) = l_0(1+\delta), \qquad \delta \equiv r^3/r_0^3.$$

The equation for l is now, from (3)

$$l^2 - 2a_0 l(1 + \varepsilon/6 + \delta) + l_0(1+\delta) = 0$$

the greater root of which, l_1, is to be compared with the greater root l_{01} of (1); we find that

$$l_1/l_{01} = 1 + (\varepsilon/3 + \delta + k\delta)/2k$$

The quantity ε, an infinitesimal of order δ, is determined from equations (2) and (3). The first equation gives

$$\varepsilon = \pm 3l^3/r_0^3$$

while elimination of ε between (2) and (3) leads to

$$(l^2 + l_0) \pm 2al = 0$$

The choice of the lower sign corresponding to $\varepsilon = -3l^3/r_0^3$, is that which leads to the correct unperturbed Störmer result (1); and so defining

$$k \equiv (1 - l_0/a_0^2)^{1/2} \equiv (1 - \cos\omega\cos^3\lambda)^{1/2}$$

we have, to first order in δ

$$\varepsilon = -3\delta(1+k)^3\sec^6\lambda$$

Thus

$$l_1/l_{01} = 1 - (1+k)\delta\{(1+k)^2\sec^6\lambda - 1\}/2k$$

and

$$P_{(\Delta H)}/P_{(0)} = \{l_{01}/l_1\}^2 = 1 + (1+k)\delta\{(1+k)^2\sec^6\lambda - 1\}/k$$

$$P_{(\Delta H)} = P_{(0)}\left[1 + \left(\frac{1+k}{k}\right)\frac{\Delta H r^3}{2M}\{(1+k)^6\sec^6\lambda - 1\}\right]$$

or

which is the general result of III D for small ΔH.

SECTION VI-REFERENCES

1. "Theory of Geomagnetic Effects of Cosmic Radiation," M. S. Vallarta, Vol. XVI, p. 89, Handbuch de Physik, (Ed. S. Flugge 1961).

2. Physics of the Aurora and Airglow, J. W. Chamberlain, Academic Press, New York (1961).

3. "Exponential Rigidity Spectrums for Solar-Flare Cosmic Rays," P. S. Freier, and W. R. Webber, J. Geophys. Research, 68, 1605 (1963).

4. "Enhanced Ionization of the Solar Ionosphere and Solar Corpuscular Radiation," T. Obayashi and Y. Hakura, Space Research, Ed. H. Kallmann (North Holland 1960).

5. "The Main Phase of Great Magnetic Storms," S. I. Akasofu, S. Chapman and D. Veukatesan, Journal of Geophysical Research 8, 3345 (1963).

Further references, and a more detailed presentation of some of the topics discussed in this report, may be found in the following two reports prepared under this contract (references 6 and 7):

6. "Solar Flare Hazard to Earth-Orbiting Vehicles," RAC 1395-1.

7. "Solar Flare Hazard to Earth-Orbiting Vehicles," RAC 1395-2.

8. "The Earth's Main Magnetic Field-Epoch 1955.0," H. F. Finch and B. R. Leaton, M. N. R. A. S. Geophysical Suppl. 1, 314 (1957).

9. "Cosmic Ray Cut-Off Rigidities and the Earth's Magnetic Field," J. J. Quenby, and W. R. Webber, Phil. Mag. 4, 90 (1959).

10. "The Magnetosphere and Its Boundary Layer," N. F. Ness, Second Symposium on Protection Against Radiation in Space, p. 31, NASA Sp-71 (1964).

11. "Solar Protons and Magnetic Storms in July 1961," G. F. Pieper et al, Jour. Geophys. Res. 67, 4959 (1962).

12. "On the Motion of Charged Particles in the Geomagnetic Field," E. C. Ray, Ann. Phys., 24, 1 (1963).

13. "Complete Dose Analysis of the November 12, 1960 Solar Cosmic Ray Event," A. J. Masley and A. D. Goedeke, Third International Space Science Symposium, Washington, Life Sciences and Space Research, p. 95 (1962).

14. "The Effect of Charged Particle Environments on Manned Military Systems," F. L. Keller and R. G. Pruett, Second Symposium on Protection Against Radiation in Space, NASA SP-71, p. 265 (1964).

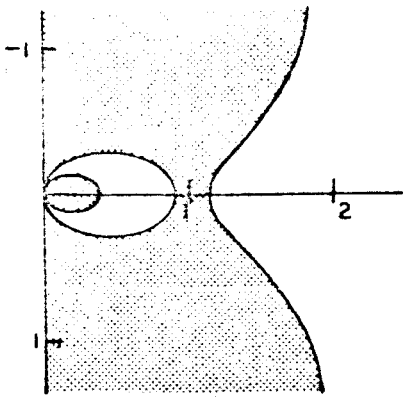

$\gamma = 1.01$

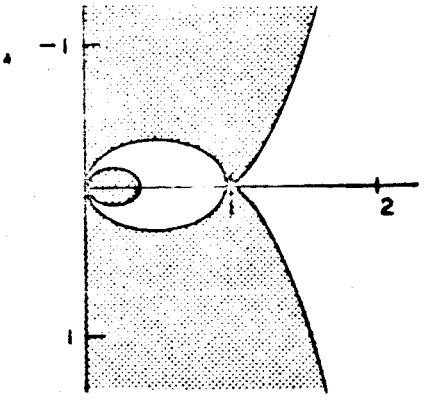

$\gamma = 1$

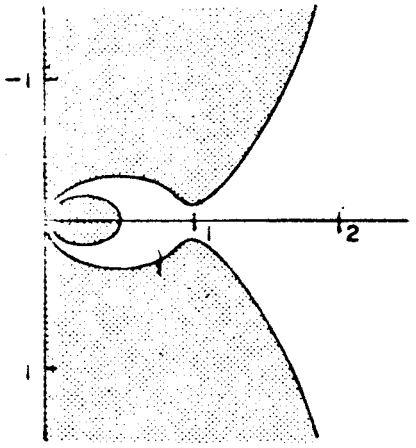

$\gamma = 0.99$

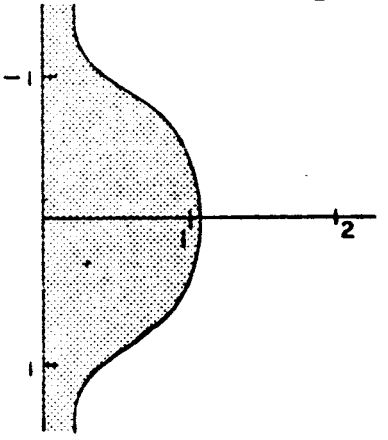

$\gamma = -0.1$

Figure I. Störmer Diagrams

Figure I shows allowed (clear) and forbidden (shaded) regions in the meridian plane for the case of a pure dipole field, and for different values of the Störmer constant γ.

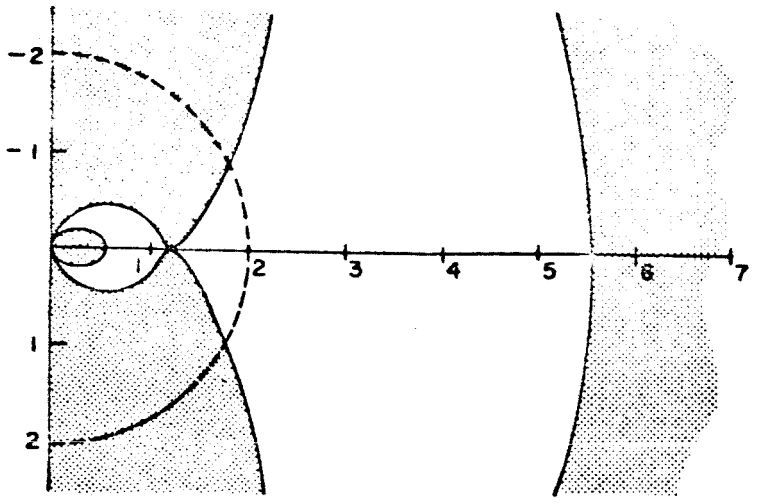

(i) Initial Phase

$r_o = 2.00 \quad \gamma = 0.93$

$(r_o > \sqrt{3})$

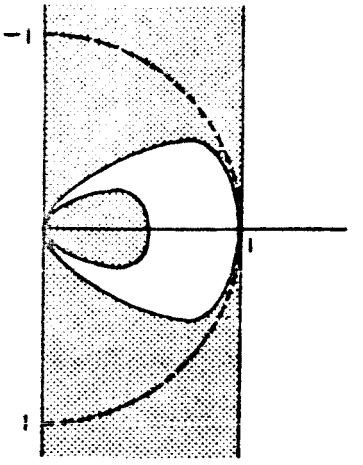

(ii) Initial Phase

$r = 1.00 \quad \gamma = 0.5$

$(r_o < \sqrt{3})$

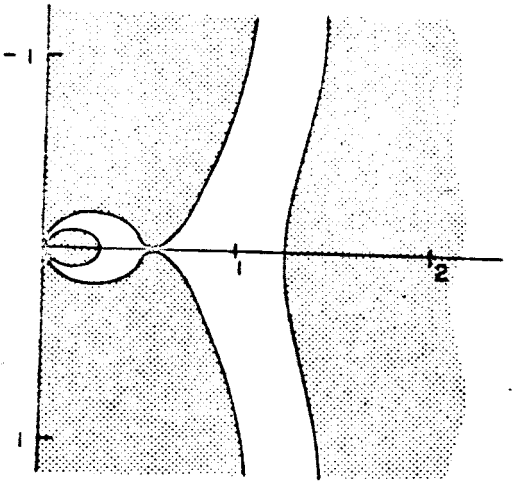

(iii) Main Phase

$r_o = -0.795$

$\gamma = 1.50$

Figure II. Modified Störmer Diagrams

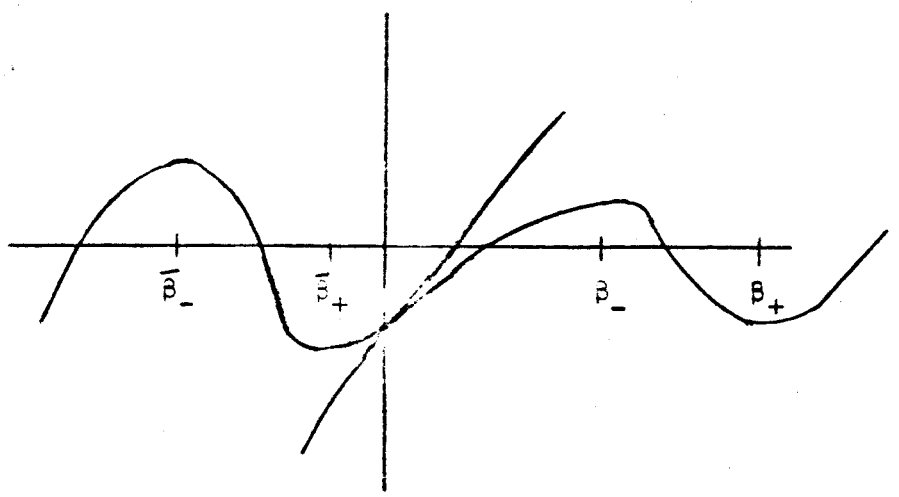

(i) Curves $f_{\pm(r)}$ for $r_o > 0$

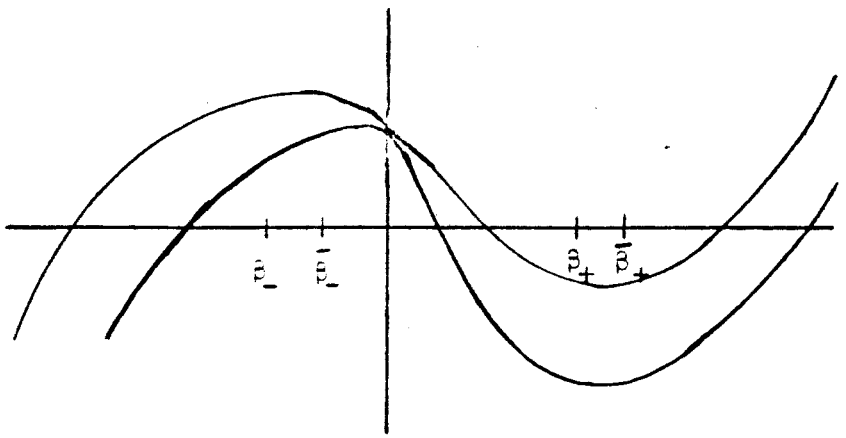

(ii) Curves $f_{\pm(r)}$ for $r_o < 0$

Figure III. Functions whose roots define Forbidden Region Equator Intersections

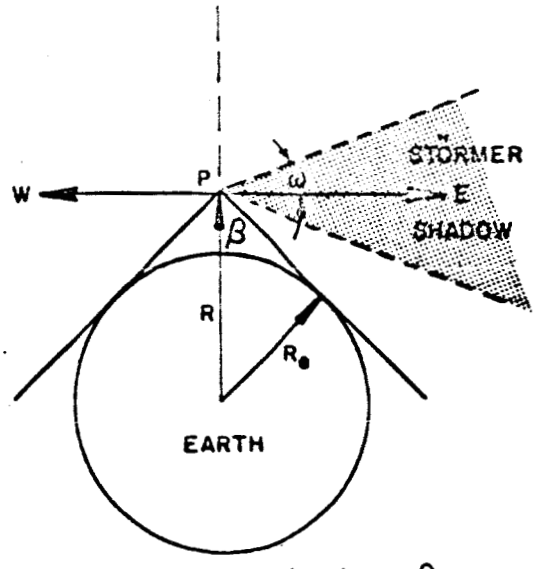

$0 \angle \omega \angle 90-\beta$

$\Omega_{ST} = 2\pi [1+\cos \omega]$

(A)

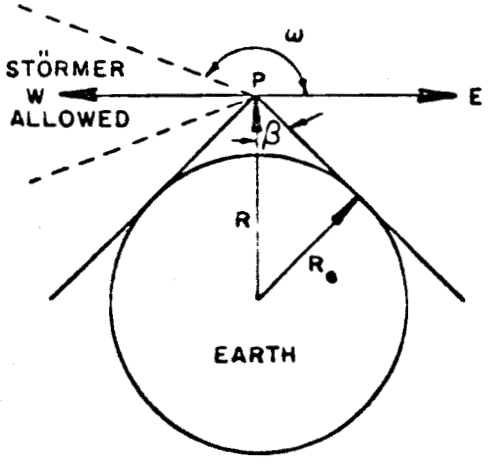

$\omega \geq 90+\beta$

$\Omega_{ST} = 2\pi [1+\cos \omega]$

(B)

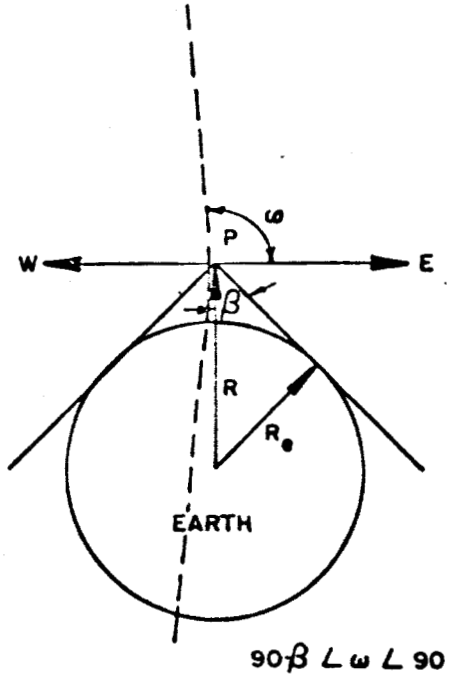

$90\beta \angle \omega \angle 90+\beta$

$\Omega_{ST} = 2\pi [1+\cos \omega]$

(C)

Figure IV. Störmer Cone and Earth Shadow Diagrams

GRAPHS

The following graphs are the results of numerical computations, using the three parts of the program, on the following mission:

Trajectory	(a)	Circular earth-orbit
	(b)	200 statute mile altitude, $r = 1.050\ r_e$
	(c)	70° geographic inclination - 82° geomagnetic (Max)
	(d)	70° geographic inclination - 58° geomagnetic (Min)
Environment	(a)	23 February 1956 Flare
	(b)	12 November 1960 Flare
Vehicle System	(a)	1.0 meter radius spherical shell, 1.0 cm aluminum skin, tissue dose point at center.
	(b)	eccentric shell, 1.01 meter radius external sphere, 1.005 meter radius inner tangential sphere, aluminum skin, tissue dose point at center of inner sphere.

Graphs

1a	$J_o(t)$, $P_o(t)$ and $\Delta H(t)$ for Storm of 23 February 1956
1b	$J_o(t)$, $P_o(t)$ and $\Delta H(t)$ for Storm of 12 November 1960
2a	Dose Rates - February Storm, Maximum and Minimum Orbits, Vehicle System (a)
2b	Dose Rates - November Storm, Maximum and Minimum Orbits Vehicle System (a)

TABLE IV

Comparative Dose Rates

Weight and dose ratios for the non-concentric system (b) as a fraction of those for the concentric system (a), for a given flux environment and various geomagnetic latitudes. The figure of merit $\rho = 1/(\text{weight ratio} \times \text{dose rate})$ is a measure of the shielding effectiveness of the system (b) compared to that of system (a) in the given environment.

Latitude	Weight Ratio (b/a)	Dose Ratio (b/a)	Figure of Merit ρ
0	.5	1.0	2.0
30	.5	1.0	2.0
40	.5	1.0	2.0
50	.5	1.0	2.0
60	.5	.95	2.1
65	.5	.94	2.1
70	.5	1.12	1.8
80	.5	1.12	1.8
90	.5	1.12	1.8

FEBRUARY FLARE

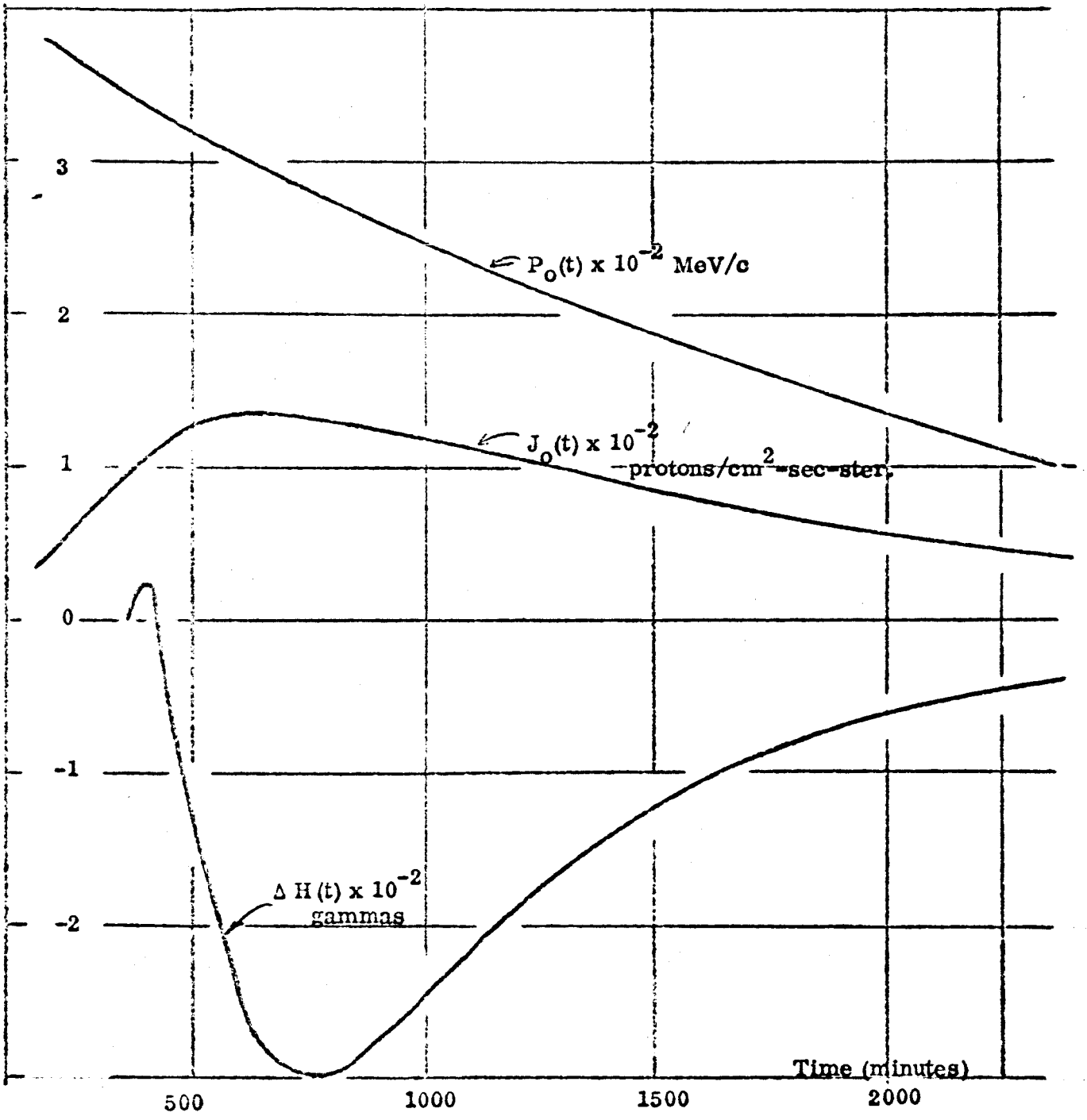

Graph 1a. Environment Due to February Flare

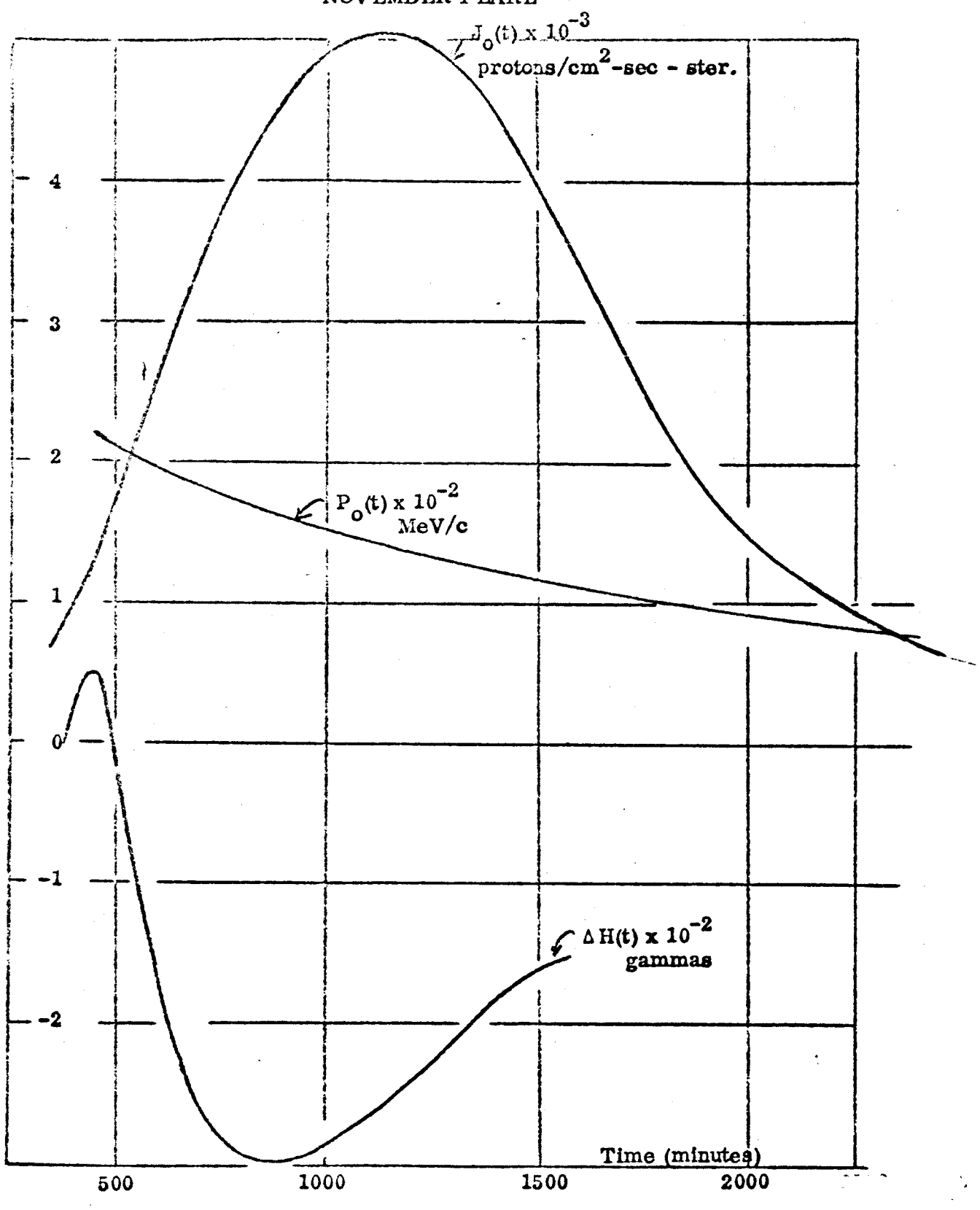

Graph 1b. Environment Due to November Flare

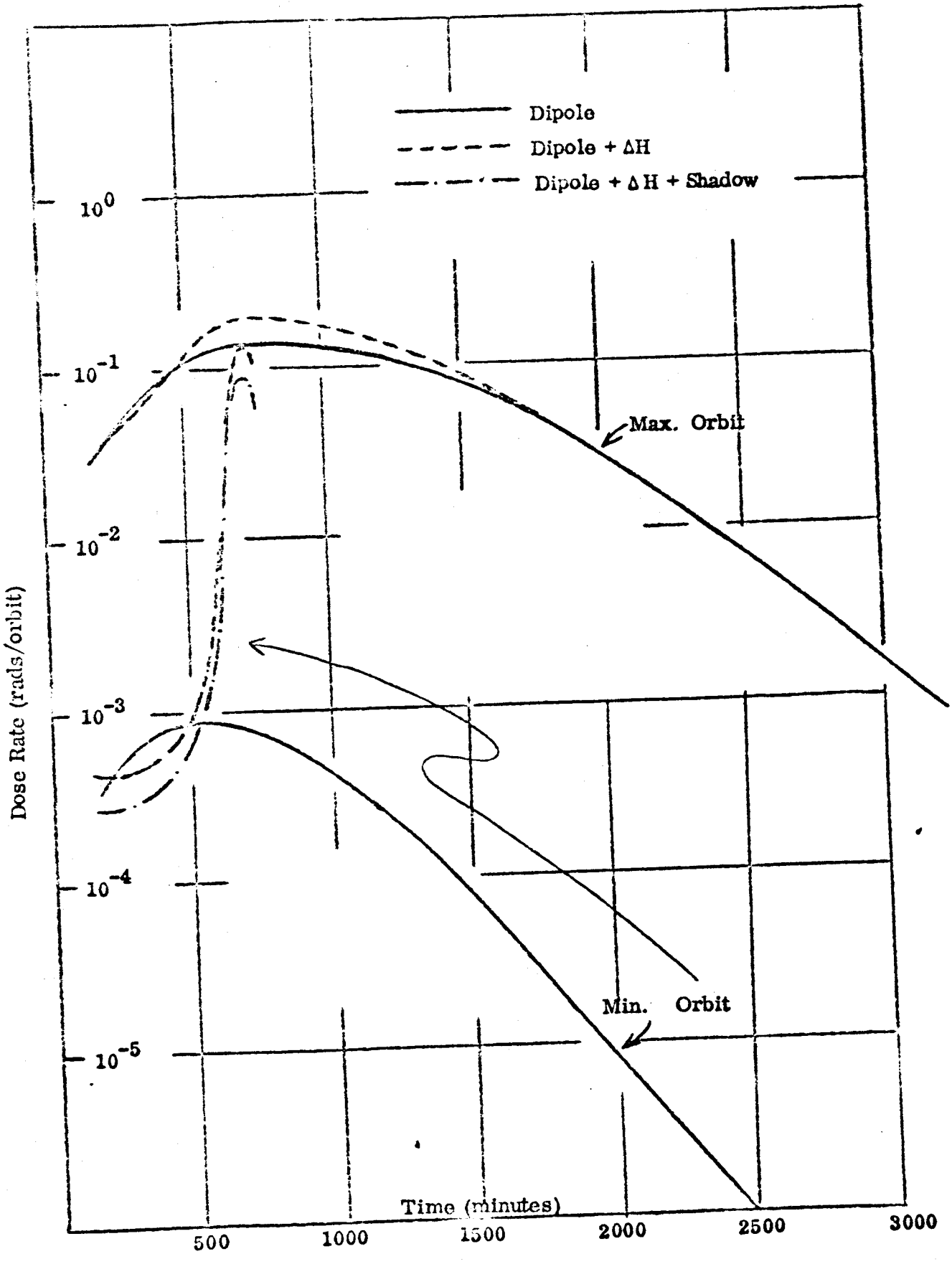

Graph 2a . Dose Rates - February Flare

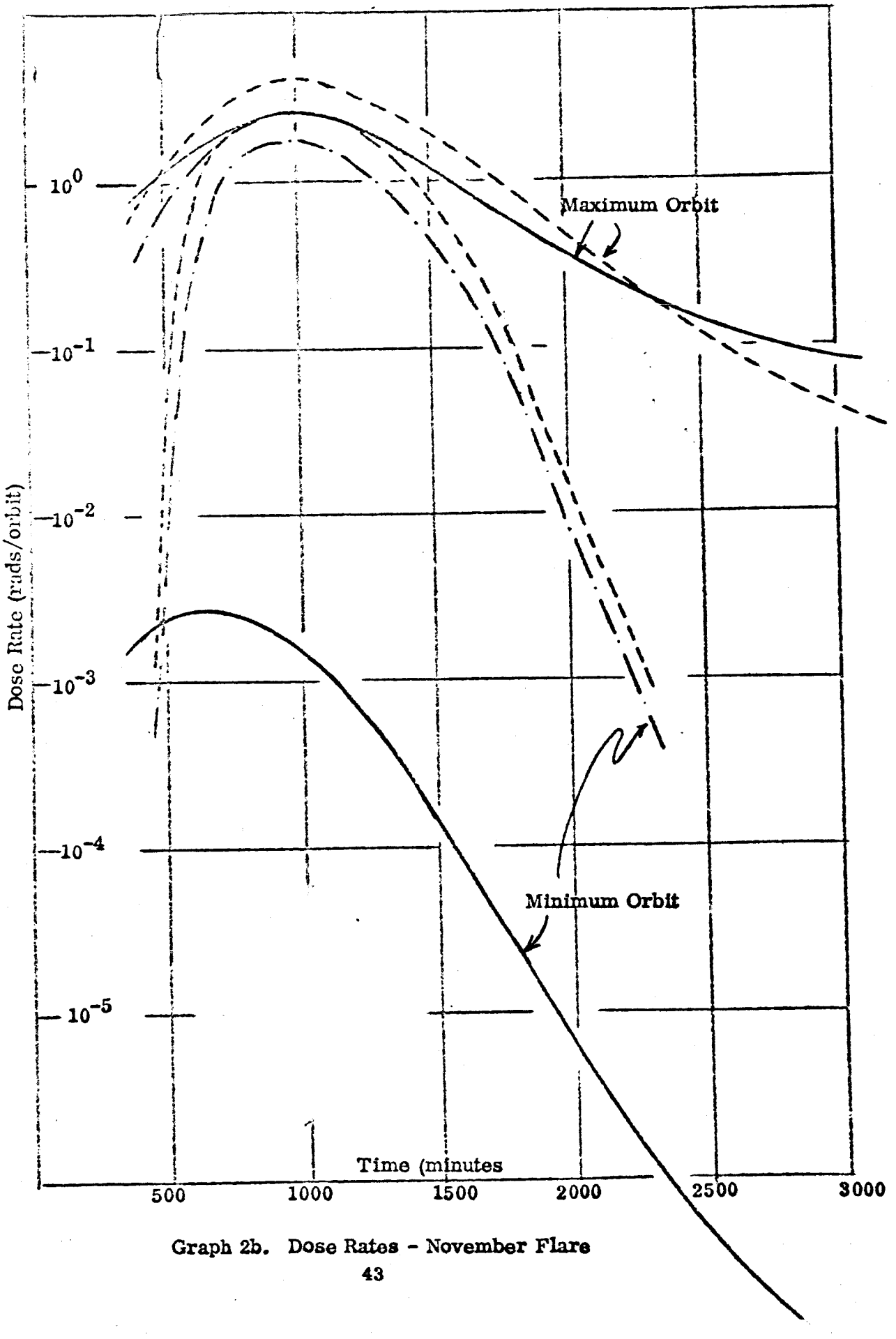

Graph 2b. Dose Rates - November Flare